

---

# Dye dispersion in the surf zone: measurements and simple models

---

Linden B. Clarke<sup>1</sup>, Drew Ackerman and John Largier<sup>2</sup>

## ABSTRACT

To examine the spatial and temporal effect of low-volume land-based runoff on beach contamination, discrete batches of dye were released at the shoreline at three beaches in Santa Monica Bay in 2000 (Malibu Creek, Santa Monica Canyon and Pico Kenter drain). Dye concentration was measured at the shoreline 25, 50, and 100 m alongshore from the dye release point for up to 40 minutes after dye release. The shoreline concentration time series are characterized either by approximately exponential decay in concentration after passage of the dye patch maximum concentration or by persistent low concentration up to 30 minutes after passage. Preprint submitted to Elsevier Science, December 1, 2006 of the initial dye patch front. In the absence of detailed measurements of physical conditions, several simple advection-diffusion models are used to simulate shoreline concentration time series for an idealized surf zone in order to probe the roles of alongshore current shear and rip currents in producing the observed characteristics in dye concentration time series. Favorable qualitative and quantitative comparison of measured and simulated time series suggest alongshore current shear and rip currents play key roles in generating the observed characteristics of nearshore dye patch dispersion. The models demonstrate the potential effects of these flow features on the extent and duration of beach contamination owing to a continuous contamination source.

## INTRODUCTION

Studies of fecal indicator bacteria contamination of Southern Californian shorelines invariably point to river, creek, storm drain, or lagoon sources (Noble *et al.* 2000, Grant *et al.* 2001, Schiff *et al.* 2003) or to shallow groundwater discharge (Boehm *et al.* 2004). Effluent entrained in nearshore water circula-

tion is mixed and transported by waves and currents away from discharge points potentially impacting remote beaches. The complexity of nearshore circulation, rudimentary understanding of factors governing dilution and trajectory of contaminant plumes in the surf zone and the difficulty of predicting the extent of coastline impacted by drain and river outflows continue to challenge water quality monitoring and beach management agencies.

Analysis of observations from state mandated shoreline water quality monitoring at drains and beaches in Santa Monica Bay, Southern California, show the frequency and extent of beach contamination owing to exceedance of water quality thresholds for indicator bacteria during dry weather (Apr-Oct) is twice that for wet weather (Nov-Mar; Schiff *et al.* 2003). Furthermore, the potential risk to human health is compounded by the large and disproportionate number of beach goers during the dry summer months. Consequently dilution rates, residence time and extent of beach contamination near outflow sources is a prime concern during periods of low drain and river discharge where inertia of outflow into the surf zone is insignificant and effluent is rapidly entrained by ambient nearshore currents.

An idealized nearshore circulation cell has been defined as the region between two adjacent rip currents and spanning the surf zone width to some distance beyond the breakers (Shepard and Inman 1951, Inman *et al.* 1971). Rip currents are fed by alongshore currents and water ejected from the surf zone by rips is gradually reintroduced to the surf zone through the breaker region. Although this pattern is frequently observed in nature, prediction of water parcel trajectory is frustrated by variability introduced by sporadic pulsing of rip currents (Smith and Largier 1995), variation in alongshore position of rip

---

<sup>1</sup> Oregon State University, College of Oceanic and Atmospheric Sciences, Corvallis, OR

<sup>2</sup> University of California, Davis, Bodega Marine Laboratory, Bodega Bay, CA

currents when unconstrained by bathymetric cross-shore channels (Murray and Reydellet 2001), meandering or eddy-shedding alongshore currents, reversal of alongshore current direction and change in flow pattern induced by change in tidal water level at barred beaches (Schmidt 2003).

Hydrodynamic models have been used to simulate nearshore flow fields that are both complex and time-varying (Allen *et al.* 1996, Slinn *et al.* 1998, Ozkan-Haller and Kirby 1999) but comparison with field observations (Schmidt 2003) suggest that although general trends in modeled circulation may be valid, prediction of time-varying water parcel trajectories remains challenging in the surf zone. Furthermore, these models are computationally expensive, require well defined boundary conditions, bathymetry and estimates of parameters such as friction factor and mixing coefficients.

Consequently, research directed at quantifying the extent of beach impacted by a contaminant source has typically adopted simplified flow fields; primarily depth-averaged alongshore current defined using measurements of incident waves (Grant *et al.* 2005, Boehm *et al.* 2005, Boehm 2003) or wind (Stretch and Mardon 2005). Bulk parameterization of dispersion in the surf zone along coastline lengths  $O(10 \text{ km})$  integrates the effects of smaller scale mixing and transport processes owing to fluid motions such as rip currents and eddies, and of flow characteristics such as current shear. Individually, these phenomena have been well studied but their roles in surf zone dispersion have received less attention.

During 1999-2000, 14 dye release experiments were conducted at several beaches in Santa Monica Bay, Southern California with the purpose of assessing the dispersion of low-volume discharges released at the shoreline. This paper describes the measurements and analysis in which four simple models are used to estimate along-shore and cross-shore dispersion coefficients and to explore the role of two dominant flow properties hypothesized to be responsible for distinct characteristics observed in measurements of dispersing dye patches: alongshore current shear (i.e., cross-shore shear in the alongshore current), and rip currents. The models are extended to explore the effect of rip currents on the region of beach impacted by effluent outflows.

## METHODS

### Beach Sites and Field Methods

Field work reported in this paper was conducted between November 11, 1999 and July 9, 2000 on three beaches in Santa Monica Bay adjacent to river or drain outlets (Figure 1). Malibu Creek feeds a lagoon and drains onto Surfrider beach which faces (direction of shore-normal)  $\sim 130^\circ$  from North and is located  $\sim 450 \text{ m}$  west of Malibu Pier. The intertidal beach is a mixture of sand and large cobbles. Waves break offshore on a sand/rock bar with a secondary break near the shore. The shallow channel connecting the lagoon and surf zone was open during all field episodes. Santa Monica Canyon drains from a concrete channel onto Will Rogers State Beach approximately  $2.6 \text{ km}$  northwest of Santa Monica Pier. The beach in this region faces  $\sim 220^\circ$ . Pico Kenter storm drain channel is located approximately  $500 \text{ m}$  south of Santa Monica Pier where the beach faces  $\sim 235^\circ$ . Santa Monica Canyon and Pico Kenter drain outflows form sandy channels across the beach but during low discharge the channel outlet cut into the foreshore slope may be blocked by redevelopment of beach crest. Mean beach slope between swash and breakpoint was measured at Malibu Creek (0.07), Santa Monica Canyon (0.09) and Pico Kenter drain (0.07) on May 4, 2000 using a transit and a 13-foot staff.

Discrete dye release experiments were conducted at Malibu Creek, Santa Monica Canyon and Pico Kenter drain (Table 1). Fluorescein was chosen over Rhodamine WT to minimize public concern over the dye release on these heavily used beaches and to minimize the persistence of dye in the surf zone after the experiments. The exponential decay rate of

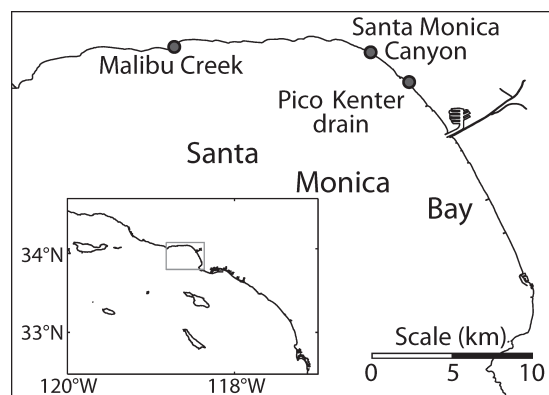


Figure 1. 1999 and 2000 shoreline dye study sites in Santa Monica Bay.

**Table 1. Batch dye release dates, locations and dye quantity (ml 30% by mass sodium fluorescein).**

| Date     | Malibu Creek    | Santa Monica Canyon | Pico Kenter     |
|----------|-----------------|---------------------|-----------------|
| 03/16/00 |                 | 35                  | 35              |
| 03/28/00 | 25              | 35                  | 35              |
| 04/04/00 | 25              | 35                  | 35              |
| 04/25/00 | 20              | 35                  | 25              |
| 05/04/00 | 30              | 40                  | 25              |
| 05/24/00 | 35              | 50                  |                 |
| 06/07/00 | 30 <sup>a</sup> |                     | 40 <sup>a</sup> |

<sup>a</sup> Shoreline and offshore samples

fluorescein exposed to sunlight has been estimated as 0.1 hr<sup>-1</sup> (Smart and Laidlaw 1977). For the present beach experiments, typical exponential decay rate of dye patch maximum concentration was ~50 hr<sup>-1</sup>. Photobleaching over the 40-minute sampling interval was estimated to introduce an error of seven percent in concentration measurements.

The direction of alongshore current was visually determined prior to pouring 25 - 50 ml of 30% by mass liquid fluorescein dye into the sea from about 0.3 m above the surface where drain discharge contacted the swash. The dye container was rinsed once with sea water. Personnel stationed at fixed positions 25, 50, and 100 m downdrift from the release point collected water samples in ~0.3 m depth in 100 ml nalgene bottles at 30- or 60-second intervals for up to 40 minutes after dye release. Fluorescein concentration was determined in the laboratory using a Turner 10-AU fluorometer. On 06/07/00 at Malibu Creek and Pico Kenter drain water samples were collected concurrently at fixed positions alongshore at both the shoreline and within 5 m of initial wave breaking (breaker line) in water depth ~1.5 m. In the absence of any fluorescein dye, background fluorescence values were equivalent to ~0.1 ppb.

### Physical Conditions

Insufficient measurement of local physical conditions at each beach site during field work precluded a detailed analysis of their possible relationship to variations in dye dispersion. Although measurements of deep water significant wave height, period and direction (from National Data Buoy Center Station 46025 located 33 NM WSW of Santa Monica, California) describe the regional wave field,

reliable estimates of nearshore wave characteristics were precluded owing to effects such as shadowing by Santa Barbara Channel islands and refraction of shoaling waves over unmeasured nearshore bathymetry. A cursory analysis of beach slope measurements and deep water wave characteristics provided some basis for comparing beach sites according to angle of wave incidence and surf zone width.

Surf zone width,  $W$ , (a parameter used in subsequent models) was estimated by:

$$W = \frac{d_b}{S}, d_b = \frac{0.39g^{0.2}(TH_\infty^2)^{0.4}}{\gamma} \quad (1)$$

where  $d_b$  is water depth in which waves break,  $g$  is acceleration due to gravity,  $T$  is wave period,  $H_\infty$  is deep water wave height,  $\gamma \approx 1$  (Komar 1998),  $W$  is surf zone width (distance from shoreline to breaker line) and  $S$  is beach slope.

Estimates of  $W$  (Table 2) are consistent with observations from field notes and measured distance to offshore sample stations located near the breaker line at Malibu Creek and Pico Kenter drain. The surf zone was generally narrower at Pico Kenter drain where the waves collapsed onto the shoreface during high tide rather than breaking offshore. Potentially stronger alongshore currents suggested by higher estimated angle of incidence at Pico Kenter drain compared to Santa Monica Canyon are generally not apparent in measured dye patch advection velocities at the two sites (Table 3). Angle of wave incidence at Malibu Creek frequently exceeds 90° owing to the protruding beach around the lagoon entrance resulting in extreme wave refraction. Sand bars were occasionally noted at Santa Monica Canyon and Malibu Creek.

### Observations from Discrete Dye Release Measurements

Dye dilution factors ( $C(0, 0)/C(y, t)$ , where  $C$  is dye concentration,  $y$  is alongshore distance from dye release, and  $t$  is time since dye release) ranged between  $4 \times 10^5$  and  $4 \times 10^7$  at  $y = 25$  m,  $2 \times 10^6$  and  $2 \times 10^8$  at  $y = 50$  m, and  $1 \times 10^7$  and  $2 \times 10^8$  at  $y = 100$  m. However, dilution 100 fold or more might be accounted for by initial mixing during the poured dye release. Dye dilution at Malibu Creek, Pico Kenter drain, and Santa Monica Canyon varied by a factor of 10 with Malibu Creek being lowest and Pico Kenter drain highest (Figure 2).

**Table 2. Physical conditions at Malibu Creek (MC), Santa Monica Canyon (SMC), and Pico Kenter drain (PK). Deep water significant wave height ( $H_\infty$ ); period ( $T_p$ , peak and average); and direction (Dir., from National Data Buoy Center Station 46025). Computed angle of wave incidence ( $\alpha$ , relative to shore normal) and surf zone width ( $W$ ).**

| Date     | Beach | $H_\infty$ (m) | $T_p/T_a$ | Dir. (°) | $\alpha$ (°) | $W$ (m) |
|----------|-------|----------------|-----------|----------|--------------|---------|
| 03/28/00 | MC    | 1.3            | 18.6/8.7  | 252      | 122          | 34/25   |
| 04/04/00 | MC    | 0.9            | 14.7/5.6  | 228      | 098          | 25/17   |
| 04/25/00 | MC    | 1.3            | 9.8/7.3   | 271      | 141          | 27/24   |
| 05/04/00 | MC    | 1.0            | 9.3/6.7   | 250      | 120          | 22/20   |
| 05/24/00 | MC    | 1.1            | 15.4/10.6 | 207      | 077          | 29/25   |
| 06/07/00 | MC    | 1.1            | 16.7/6.3  | 200      | 070          | 23/15   |
| 03/28/00 | SMC   | 1.3            | 19.5/7.5  | 252      | 032          | 35/24   |
| 05/04/00 | SMC   | 1.0            | 15.4/7.2  | 212      | -08          | 26/19   |
| 05/24/00 | SMC   | 1.1            | 15.7/10.6 | 206      | -14          | 28/24   |
| 03/28/00 | PK    | 1.3            | 19.5/7.1  | 253      | 018          | 23/15   |
| 04/04/00 | PK    | 0.9            | 14.7/5.6  | 228      | -07          | 16/11   |
| 05/04/00 | PK    | 0.9            | 15.1/7.0  | 213      | -22          | 16/12   |
| 06/07/00 | PK    | 1.2            | 16.7/6.4  | 204      | -31          | 31/21   |

The profiles of measured concentration time series (Figures 3 - 5) can generally be described in three segments; the ramp up to peak concentration, peak duration and ramp down from peak concentration.

**Table 3. Alongshore current velocity =  $v$  ( $m\ s^{-1}$ ), estimated using alongshore distance between dye release and sample position ( $y$ ) and elapsed time from dye release to arrival of concentration peak at sample position.**

| Date     | Beach | $v$         |             |              |
|----------|-------|-------------|-------------|--------------|
|          |       | $y = 25\ m$ | $y = 50\ m$ | $y = 100\ m$ |
| 03/28/00 | MC    | 0.08        | 0.10        | 0.11         |
| 04/04/00 | MC    | 0.42        | 0.56        | 0.28         |
| 04/25/00 | MC    | 0.42        | 0.43        | 0.24         |
| 05/04/00 | MC    | 0.31        | 0.22        | 0.26         |
| 05/24/00 | MC    | 0.09        | 0.10        | 0.12         |
| 06/07/00 | MC    | 0.17        | 0.21        | 0.26         |
| 03/16/00 | SMC   | 0.42        | 0.42        | 0.42         |
| 03/28/00 | SMC   | 0.09        | 0.17        | 0.08         |
| 04/25/00 | SMC   | 0.18        | 0.16        | 0.15         |
| 05/04/00 | SMC   | 0.25        | 0.25        | 0.15         |
| 05/24/00 | SMC   | 0.25        | 0.19        | 0.07         |
| 03/16/00 | PK    | 0.17        | 0.24        | 0.28         |
| 03/28/00 | PK    | 0.10        | 0.15        | 0.19         |
| 04/25/00 | PK    | 0.15        | 0.15        | 0.16         |
| 05/04/00 | PK    | 0.21        | 0.19        | 0.19         |
| 06/07/00 | PK    | 0.33        | 0.23        | 0.17         |

In all but two cases (Santa Monica Canyon 3/28/00 and 5/24/00; Figure 4b and e) the arrival of dye patch at all sample stations is marked by a sharp concentration front, the front steepness generally decreasing with greater sample station distance alongshore. Peak duration and ramp down from peak concentration appear related; brief peaks ( $O(5\ min)$ ) being followed by concave decay in concentration (for example, Figure 3c,  $y = 100\ m$ ); protracted peaks ( $O(10 - 20\ min)$ ) being followed by convex decay in concentration (for example, Figure 4d,  $y = 100\ m$ ). Although deceleration of alongshore current is likely to prolong the concentration peak at a sample station, alongshore current velocity estimated from time between concentration peak arrival at subsequent stations suggests that this mechanism is not responsible for the protracted peaks observed. Furthermore, in these cases concentration at 100 m remains relatively constant for periods of 20 - 30 minutes despite non-zero alongshore flow. This behavior is not observed at 25 m but occasionally at 50 m. In some cases, multiple concentration maxima observed at 25 m persist at 50 m and 100 m (for example, Figures 3b - c and 5b). In three cases at Pico Kenter drain, observations record dye mass being transported into water deeper than the sampling depth just updrift of the sample station and subsequent onshore transport of the dye patch by breaking waves down-drift of the sample station. This resulted in peak dye concentration increase rather than decrease at downstream sample stations (Figure 5a, 25 m and 50 m; Figure 5b, 50 m and 100 m; Figure 5d, 50 m and 100 m).

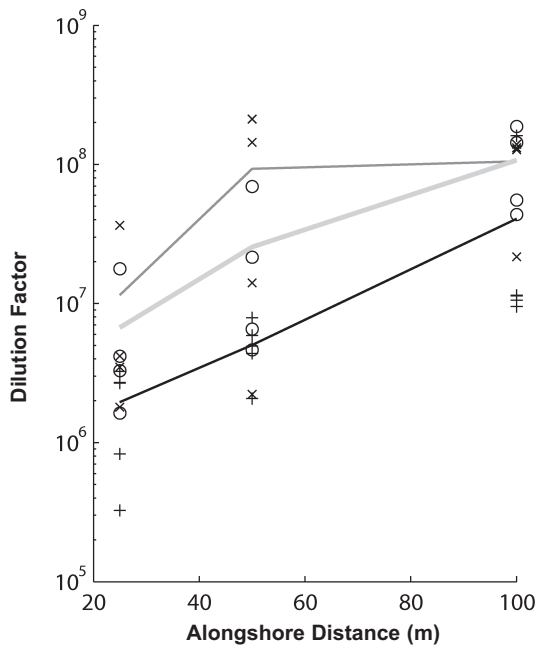


**Figure 2.** Dilution at alongshore distance  $y = 25, 50,$  and  $100$  m for each beach site. Symbols mark each dye release, lines mark site-mean. Malibu creek (+, black line), Pico Kenter drain (x, gray line), Santa Monica Canyon (O, thick light gray line). Dilution factor = initial concentration/maximum concentration at  $y$ .

### Rip Currents

The presence and alongshore position of rip currents were logged during experiments. In seven dye release events a significant decrease in concentration was recorded between two adjacent stations. This decrease coincides with visual observations of dye being transported offshore at a position between the two stations in five of these episodes (Table 4). Concentration also decreased significantly between 50 - 100 m at Pico Kenter drain (04/25/00) and 50 - 100 m at Santa Monica Canyon (05/24/00) without recorded visual observation of rip currents.

### Offshore Water Samples

On June 7, 2000, at Malibu Creek and Pico Kenter drain, water samples were also collected just beyond the breakers (Malibu Creek, 15 - 20 m offshore; Pico Kenter drain, 15 - 32 m offshore) at stations from 0 - 100 m along the beach at 25-m spacing. In both cases an alongshore current was present and only trace concentrations of dye were observed beyond the breakers adjacent to the release point. From 25 - 100 m alongshore, both the concentration maximum and the difference between the concentration at the shoreline and outer edge of the surf zone gradually decreased (Figures 6 and 7). Only at 100 m alongshore were

the shoreline and breaker line concentrations approximately equivalent with any temporal consistency. At 100 m alongshore at Pico Kenter drain, breaker line concentration exceeded shoreline concentration by up to 10 ppb. Although breaker line samples were not collected long enough to confirm the time after release when no dye was measurable, at both sites lingering low dye concentrations were found at the shoreline at distances 100 m alongshore.

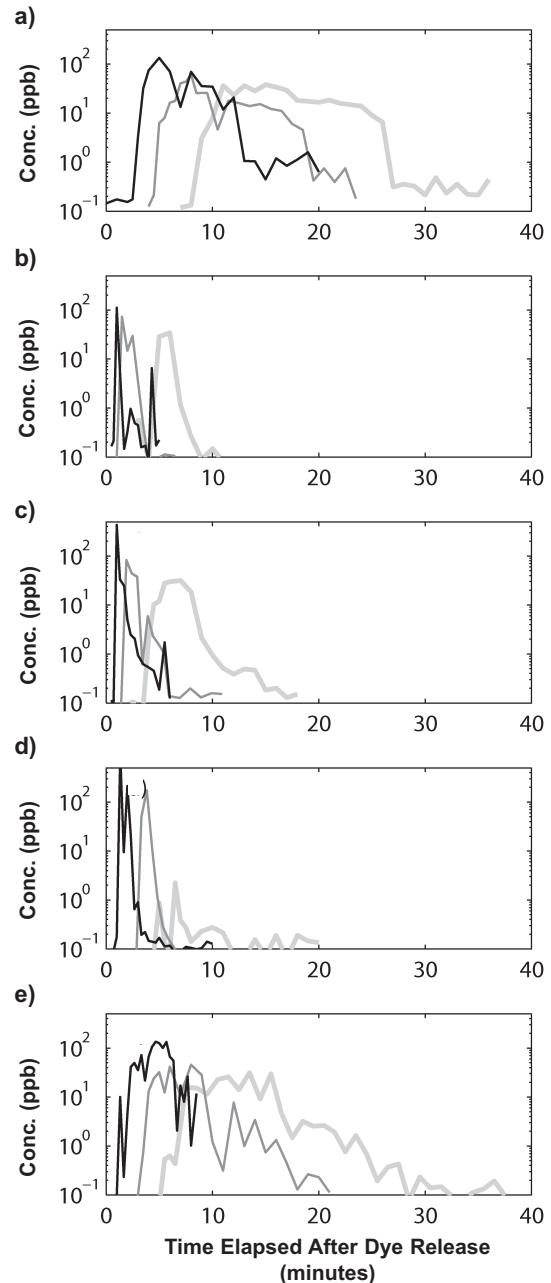


**Figure 3.** Discrete dye releases at Malibu Creek. Shoreline dye concentration at position 25 m (black line), 50 m (gray line), and 100 m (thick light gray line) alongshore from dye release point: 03/28/00 (a); 04/04/00 (b); 04/25/00 (c); 05/04/00 (d); and 05/24/00 (e). Background fluorescence values equivalent to  $\sim 0.1$  ppb.

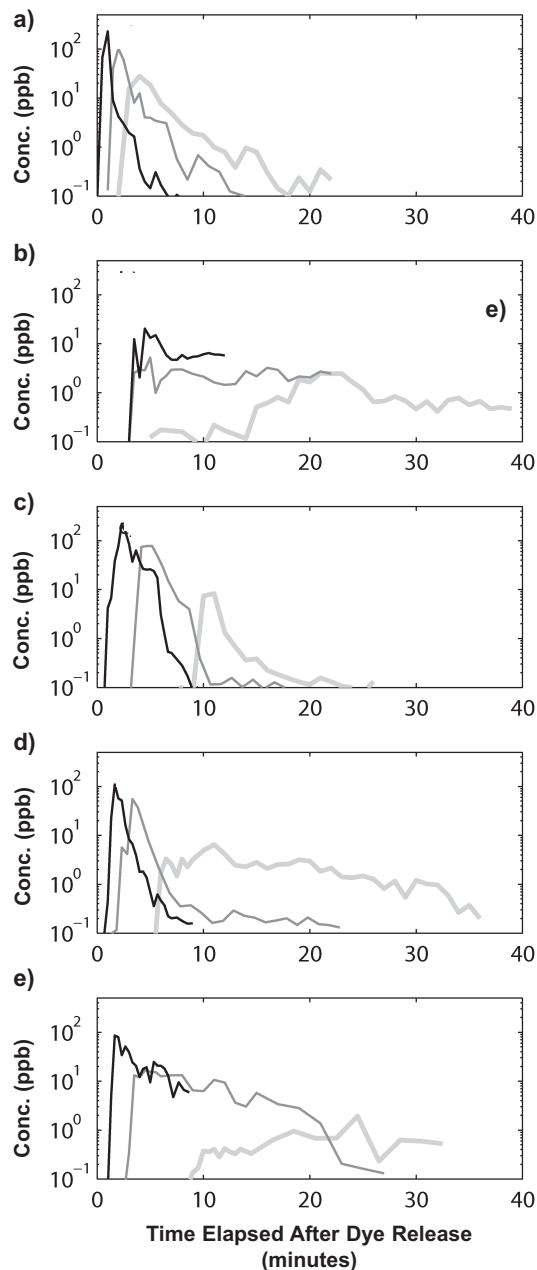


**Figure 4. Discrete dye releases at Santa Monica Canyon. Shoreline dye concentration (Conc.) at position 25 m (black line), 50 m (gray line), and 100 m (thick light gray line) alongshore from dye release point: 03/16/00 (a); 03/28/00 (b); 04/25/00 (c); 05/04/00 (d); and 05/24/00 (e).**

### Comparison of Shoreline Concentration Time Series

Qualitative comparison of shoreline dye concentration time series from different dye release episodes and beaches suggests two general categories for dye patch dispersion. In the first category, shoreline concentration is characterized by a sharp rise ( $O(1 \text{ min})$ ) to a well defined, narrow peak followed by rapid decay ( $O(5 - 10 \text{ min})$ ) and definite

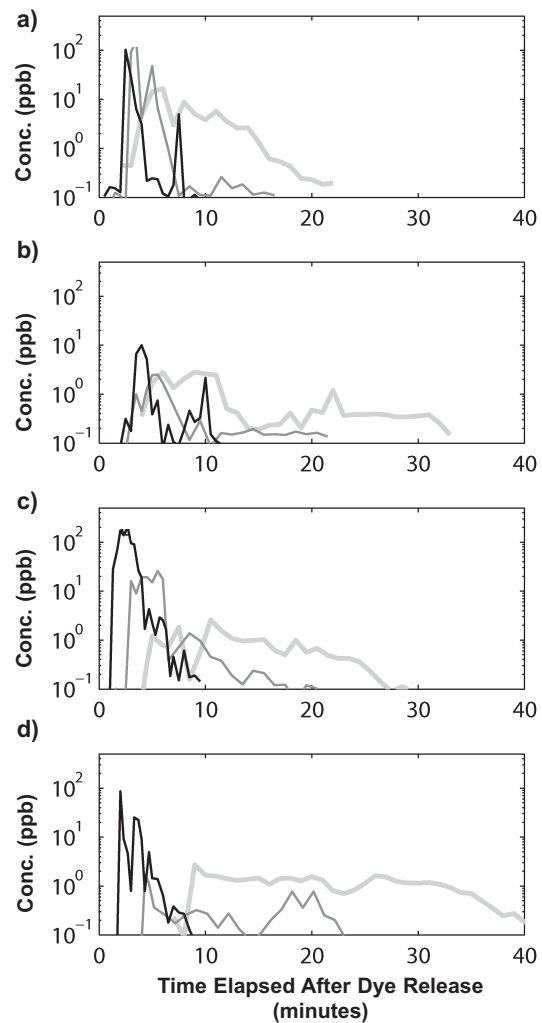


**Figure 5. Discrete dye releases at Pico-Kenter drain. Shoreline dye concentration (Conc.) at position 25 m (black line), 50 m (gray line), and 100 m (thick light gray line) alongshore from dye release point: 03/16/00 (a); 03/28/00 (b); 04/25/00 (c); and 05/04/00 (d).**

termination of the trailing edge of the dye patch. At subsequent alongshore sample stations the dye patch exhibits a similar temporal profile but with a moderate reduction in peak concentration and moderate increase in patch duration. In the second category, shoreline concentration is characterized by a relatively gentle rise to peak concentration which is significantly reduced from the peak concentration at the immediate upstream sample station. The peak concentration for the dye patch is poorly defined in time and persists for an extended duration often with little variation in concentration.

According to this classification only one sample station at Malibu Creek ( $y = 100, m$  05/04/00) qualifies as category two whereas 50% of sample stations at Santa Monica Canyon and Pico Kenter drain qualify

**Table 4. Rip current observations during batch dye release episodes.**

| Date     | Beach | Rip Position (m) | Figure |
|----------|-------|------------------|--------|
| 05/04/00 | MC    | 50 - 100         | 3d     |
| 03/28/00 | SMC   | 0 and 66         | 4b     |
| 05/04/00 | SMC   | 70.0             | 4d     |
| 03/28/00 | PK    | 12.0             | 5b     |
| 05/04/00 | PK    | 35 and 65        | 5d     |

as category two, most of these being located 50 – 100 m from the dye release point.

All recorded observations of rip currents for the experiment coincide with category two patch dispersion characteristics and the substantial reduction in peak patch concentration occurs at stations immediately downstream of the observed rip location, suggesting that a fraction of dye mass is removed from the surf zone by entrainment in a rip current (as in Inman *et al.* 1971).

In the next three sections, the role of physical flow properties giving rise to the characteristics observed in the categorized time series are explored using several models. Progressing from a 1D advection-diffusion equation to a 2D discrete particle random walk model, alongshore current shear and rip

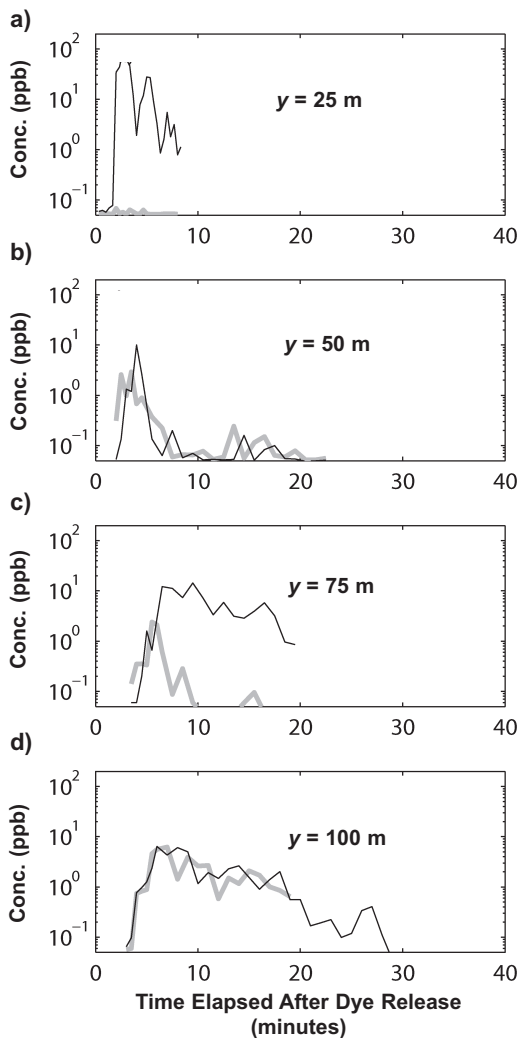


**Figure 6. Shoreline (black line) and breaker line (gray line) dye concentration at alongshore distance ( $y$ ) from dye release point ( $y = 0$  m) at Malibu Creek 06/07/00.**

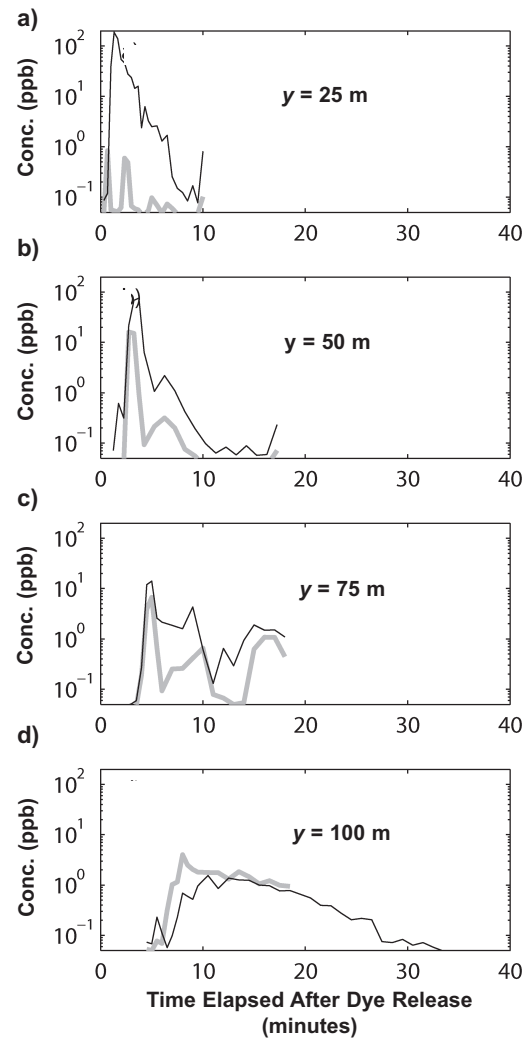


**Figure 7. Shoreline (black line) and breaker line (gray line) dye concentration at alongshore distance ( $y$ ) from dye release point ( $y = 0$  m) at Pico Kenter drain 06/07/00.**

currents are incrementally incorporated into the models as distinct properties of the flow field to examine their effect on shoreline concentration and estimated alongshore and cross-shore diffusion coefficients.

## RESULTS

### Advection-diffusion Models

Solute or particle dispersion may be modeled as an advection-diffusion process, the advection velocity across the model domain being derived from an hydrodynamic model (Sanchez-Arcilla *et al.* 1998). Forcing and boundary conditions typically required by hydrodynamic models were not measured during the dye experiments precluding simulation of surf zone circulation or discrimination of the effects of local variables on dispersion of dye patches. Instead, the effect of alongshore current shear and rip currents on dye dispersion and the resulting characteristics of shoreline concentration time series is explored diagnostically using a series of 1D and 2D advection-diffusion models in conjunction with prescribed idealized flow fields. Primary model parameters, alongshore and cross-shore diffusion coefficients, are estimated using a best fit between model and measurements. Characteristics of modeled and measured concentration time series are compared for successive models with incremental addition of new flow properties to evaluate their effects on dispersion.

First, alongshore diffusion coefficients are estimated using the analytical solution to the 1D advection-diffusion equation (absence of alongshore current shear, absence of rip currents). Second, cross-shore and alongshore diffusion coefficients are estimated using the analytical solution to the 2D advection diffusion equation (absence of alongshore current shear, absence of rip currents). Third, shoreline concentration time series are simulated using numerical solution to a 2D advection-diffusion equation with alongshore current shear. Fourth, shoreline concentration time series are simulated using a discrete particle tracking advection-diffusion model with both alongshore current shear and rip current represented in the flow field. In the model, domain  $x$  represents the cross-shore coordinate ( $x = 0$  m at the shoreline) and  $y$  the alongshore coordinate ( $y = 0$  m at the dye release position).

#### 1D advection-diffusion equation

For most dye release episodes dye concentration measurements were confined to the shoreline which

allows estimation of effective alongshore diffusion using a 1D advection-diffusion model (Equation 2) in which the surf zone is idealized as a uniform flow confined by parallel boundaries at the shoreline and breaker line (imagined to be well defined and a constant distance offshore). Diffusion is assumed to be Fickian (tracer flux proportional to gradient in tracer concentration). The model predicts a Gaussian alongshore distribution of dye and implies that dye is uniformly mixed across the width of the flow (surf zone) with no flux of tracer across the surf zone boundaries.

$$C(y, t) = \frac{M}{A\sqrt{4\pi D_y t}} \exp -\frac{(y - (y_0 + vt))^2}{4D_y t} \quad (2)$$

where  $C(y, t)$  is dye concentration (as  $\text{kg m}^{-3}$ ) at alongshore position  $y$  and time  $t$ ,  $M$  is the mass of dye released at  $y_0$ ,  $A$  is the surf zone cross-sectional area,  $D_y$  is alongshore diffusion coefficient and  $v$  is alongshore current velocity.  $A$  is calculated using estimated mean surf zone width and measured beach slope (Table 2). The choice of no-flux boundary at the breaker-line was based on field observations from this and other studies suggesting that, in the absence of rip currents, dye diffusion and transport is largely confined shoreward of the region of wave breaking (Harris *et al.* 1963, Inman *et al.* 1971).

In each experiment, dye is released very close to the shoreline ( $x \approx 0$  m). The time scale for mixing to disperse dye uniformly across the flow width is  $O(W^2/4D_x)$ , where  $W$  is the surf zone width and  $D_x$  is the cross-shore eddy diffusivity (Inman *et al.* 1971). Assuming  $D_x \sim 1 \text{ m}^2 \text{ s}^{-1}$  (Inman *et al.* 1971, Harris *et al.* 1963) and  $W$  ranges 11 - 36 m, time for uniform cross-shore mixing ranges 0.5 - 5.5 minutes. The few dye concentration measurements at shoreline and breaker line positions indicate that concentrations are comparable at the surf zone “boundaries” occasionally at 50 m and more frequently at 100 m alongshore.

Accordingly, peak concentration,  $C_p$ , at alongshore sample stations  $y = 50$  m and  $y = 100$  m were used to estimate the effective alongshore diffusion coefficient,  $D_y$ . Noting that  $y = y_0 + vt$  when  $C_p = C$ , Equation 2 simplifies to:

$$C_p(y, t) = \frac{M}{A\sqrt{4\pi D_y t}}. \quad (3)$$

In most of the experiments  $D_y \ll 1 \text{ m}^2 \text{ s}^{-1}$  (Table 5). However, in cases where dye is likely transported

**Table 5. Alongshore diffusion coefficient  $D_y$  ( $\text{m}^2 \text{s}^{-1}$ ), estimated from decay in peak concentration (Equation 3). Bold = rip current observed upstream of sample station; italic = rip not reported but measurements indicate significant dye loss since previous sample station. Malibu Creek = MC; Santa Monica Canyon = SMC; and Pico-Kenter drain = PK.**

| Date     | Beach | $D_y$ , 0 - 50 (m) | $D_y$ , 0 - 100 (m) |
|----------|-------|--------------------|---------------------|
| 03/28/00 | MC    | 0.003              | 0.004               |
| 04/04/00 | MC    | 0.041              | 0.048               |
| 04/25/00 | MC    | 0.007              | 0.013               |
| 05/04/00 | MC    | 0.004              | <b>14.1</b>         |
| 05/24/00 | MC    | 0.014              | 0.018               |
| 03/16/00 | SMC   | 0.015              | 0.103               |
| 03/28/00 | SMC   | <b>1.2</b>         | <b>1.2</b>          |
| 04/25/00 | SMC   | 0.010              | 0.422               |
| 05/04/00 | SMC   | 0.059              | <b>1.3</b>          |
| 05/24/00 | SMC   | 0.455              | 6.25                |
| 03/28/00 | PK    | 0.009              | 0.493               |
| 04/04/00 | PK    | <b>10.5</b>        | <b>5.06</b>         |
| 05/04/00 | PK    | 0.115              | 5.95                |
| 06/07/00 | PK    | <b>54.0</b>        | <b>10.1</b>         |

out of the surf zone by rip currents with concurrent reduction in shoreline concentration, the assumption of no-flux boundaries is violated and 1D model estimates for  $D_y$  are large ( $D_y \gg 1 \text{ m}^2 \text{ s}^{-1}$ ). Excluding estimates affected by rip currents, mean estimated  $D_y$  for each beach was  $0.017 \text{ m}^2 \text{ s}^{-1}$  (Malibu Creek),  $0.12 \text{ m}^2 \text{ s}^{-1}$  (Santa Monica Canyon) and  $0.21 \text{ m}^2 \text{ s}^{-1}$  (Pico Kenter drain). These estimates of  $D_y$  should be used with caution given the scatter in results and absence of correlation with physical conditions at each site.

For comparison, estimates of diffusion coefficient in the surf zone from literature ranged  $0.2 - 0.4 \text{ m}^2 \text{ s}^{-1}$  at Inyoni Rocks, Natal, South Africa (surf zone width 20 - 30 m, breaker height  $\sim 1.2 \text{ m}$ ; Harris *et al.* 1963),  $0.08 - 0.3 \text{ m}^2 \text{ s}^{-1}$  El Moreno, Baja California, Mexico (surf zone width 5 - 7 m, breaker height 0.35 - 0.45 m) and  $2 - 6 \text{ m}^2 \text{ s}^{-1}$  at Scripps Beach, California (surf zone width 70 - 80 m, breaker height 0.6 - 0.8 m; Inman *et al.* 1971). These estimates of diffusion coefficient are non-directional whereas the estimates from the 1D advection diffusion model are for diffusion only in the alongshore direction. Given the cross-shore mass transport and rapid cross-shore mixing associated with shoreward propagating wave bores (Inman *et al.* 1971) and

the absence of equivalent processes in the alongshore direction, it is feasible that the cross-shore diffusion coefficient,  $D_x$ , might be significantly larger than  $D_y$ , and that diffusion values cited in the literature might reflect this dominance of cross-shore mixing processes.

In the 1D model, decrease in peak concentration is attributed solely to alongshore spreading of the dye patch. Consequently, at sites where offshore transport by rip currents resulted in significant decrease in shoreline concentration, the model assumption of no loss at the surf zone boundary is violated,  $D_y$  is over-estimated and the alongshore extent of the dye patch is exaggerated to account for observed dilution. At Malibu Creek, where rip currents were rarely observed, estimates for  $D_y$  at 50 m and 100 m are relatively constant compared with those at Pico Kenter drain and Santa Monica Canyon where alongshore current velocity was generally faster and rip currents more frequent.

Using the estimated alongshore current velocities and  $D_y$  for each dye release episode this very simple 1D model reproduces the peak concentration at distances 50 m and 100 m from the dye release point but models the concentration time series at those sample stations very poorly. For small  $D_y$  ( $< 0.1 \text{ m}^2 \text{ s}^{-1}$ ), the modeled dye patch is very narrow and fails to reproduce the low concentration tails frequently observed at 50 m and 100 m alongshore (Figure 8a and b) moderate  $D_y$  ( $> 0.1 \text{ m}^2 \text{ s}^{-1}$ ), the modeled dye patch is wider and in some cases approximates the long, low concentration tail but does not show the sudden arrival of a sharp patch front. Rather, the model predicts an earlier arrival time of a lower gradient front as a consequence of exaggerated alongshore extension of the dye patch (Figure 8c,  $y = 100 \text{ m}$ ). For large  $D_y$  ( $\gg 1 \text{ m}^2 \text{ s}^{-1}$ ), the modeled concentration approximates the convex low concentration tail (Figure 8d,  $y = 100 \text{ m}$ ).

The shape of the modeled concentration profile (convex or concave) after passage of the dye patch peak depends on the non-dimensional Peclet number,  $P_e$ , which characterizes relative effects of two dye transportation mechanisms; advection of the patch away from the sample station and diffusion of the patch in the opposite direction to the alongshore current.

$$P_e = \frac{D_y}{vl} \quad (4)$$

where  $v$  is the alongshore current velocity and  $l$  is the characteristic length scale (50 m). Tracer trans-

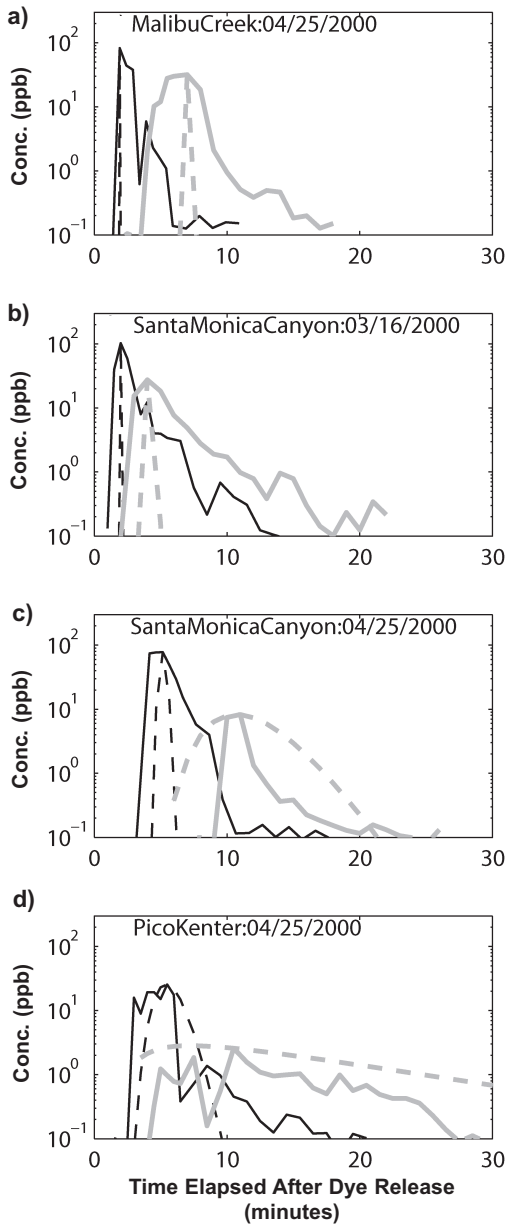


**Figure 8.** Shoreline dye concentration (Conc.) measurement (solid lines) and prediction (dashed lines) from Equation 2, at 50 m (black lines) and 100 m (gray line) alongshore from dye release:  $D_y \ll 0.1 \text{ m}^2 \text{ s}^{-1}$  (a) and (b);  $D_y \sim 0.1 \text{ m}^2 \text{ s}^{-1}$  (c); and  $D_y \gg 0.1 \text{ m}^2 \text{ s}^{-1}$  (d).

port is advection dominated for  $P_e \ll 1$  (resulting in a convex concentration tail) and diffusion dominated for  $P_e \approx 1$  or greater (resulting in a concave concentration tail). Of the 28 intervals between 50 m and 100 m sample stations, 18 are characterized as advection dominated with  $P_e < 0.1$ . Of the 10 intervals with  $P_e > 0.1$ , 8 coincide with observed interaction between the dye patch and rip currents, making their classification as diffusion dominated inconclusive.

The predicted rapid alongshore diffusion and early arrival time of the dye patch (up to 5 minutes before measurements) associated with  $D_y \gg 1 \text{ m}^2 \text{ s}^{-1}$  makes these extreme values questionable as a valid explanation of the observed long, low-concentration tails.

#### Analytical solution to the 2D advection-diffusion equation

Extending the model (Equation 2) to 2D allows for transient mixing of dye from the shoreline release point to the breakers and estimation of the cross shore diffusion coefficient  $D_x$ . A no-flux boundary condition was applied at the shoreline and breaker line.  $D_x$  is assumed constant across-shore.

$$C(x, y, t) = \frac{2M}{4\pi dt \sqrt{D_x D_y}} \sum_{i=-m}^m \exp - \left[ \frac{(x + 2iW - x_0^2)^2}{4D_x t} + \frac{(y - (y_0 + vt))^2}{4D_y t} \right] \quad (5)$$

where  $d$  is the mean surf zone depth,  $m$  is the number of imaginary dye sources used to implement the no-flux boundary conditions ( $m \approx 16$ ; Fischer *et al.* 1979),  $x_0$  is the offshore distance of dye release ( $x_0 = 0 \text{ m}$ ). Equation 6 implies zero depth-averaged cross-shore current velocity.  $D_x$  and  $D_y$  were estimated at 25, 50, and 100 m alongshore with shoreline measurements only.  $D_x$  and  $D_y$  were estimated by minimizing the RMS error between time series of predicted and measured concentrations at each shoreline sample station. Mean surf zone depth was calculated from measured beach slopes and estimated mean surf zone width; mean along shore velocity between point of dye release and sample station was estimated from elapsed time to arrival of dye patch peak concentration.

Model performance was estimated by  $R^2$ :

$$R^2(y) = 1 - \frac{\sum_{j=1}^n [C_j(y) - C'_j(y)]^2}{\sum_{j=1}^n [C_j(y) - \bar{C}(y)]^2} \quad (6)$$

where  $n$  is the number of water samples taken at alongshore distance,  $y$ , from dye release point,  $C$  is measured concentration,  $C'$  is predicted concentration and  $\bar{C}$  is mean measured concentration. Assuming that deviation of predictions from measurements are normally distributed, mean  $R^2$  at each site indicates that the model explained between 66%

**Table 6. Cross-shore ( $D_x$ ) and alongshore ( $D_y$ ) diffusion coefficients ( $\text{m}^2 \text{s}^{-1}$ ) at each alongshore sample station (25, 50, and 100 m) from least square fit of Equation 5. Bold = rip current observed upstream of sample station; italic = rip not reported but measurements indicate significant dye loss since previous sample station. Malibu Creek = MC; Santa Monica Canyon = SMC; and Pico Kenter drain = PK.**

| Date     | Beach | $D_{x25}$    | $D_{x50}$    | $D_{x100}$     | $D_{y25}$    | $D_{y50}$    | $D_{y100}$    | $R^2$        |
|----------|-------|--------------|--------------|----------------|--------------|--------------|---------------|--------------|
| 03/28/00 | MC    | 0.02         | 0.04         | 0.01           | 0.04         | 0.08         | 0.43          | 0.75         |
| 04/04/00 | MC    | 0.92         | 0.16         | 0.07           | 0.07         | 0.39         | 0.29          | 0.86         |
| 04/25/00 | MC    | 0.02         | 0.04         | 0.01           | 0.08         | 0.29         | 0.56          | 0.88         |
| 05/04/00 | MC    | 0.12         | 0.09         | <b>187.0</b>   | 0.01         | 0.03         | <b>417.0</b>  | 0.67         |
| 05/24/00 | MC    | 0.04         | 0.05         | 0.02           | 0.07         | 0.41         | 0.61          | 0.66         |
| 03/16/00 | SMC   | 0.11         | 0.06         | 0.06           | 0.19         | 0.41         | 1.35          | 0.94         |
| 03/28/00 | SMC   | <b>18.6</b>  | <b>11.7</b>  | <b>26.0</b>    | <b>0.30</b>  | <b>6.2</b>   | <b>9.36</b>   | <b>-0.5</b>  |
| 04/25/00 | SMC   | 0.08         | 0.05         | <i>2470.00</i> | 0.07         | 0.13         | <i>0.05</i>   | 0.83         |
| 05/04/00 | SMC   | 0.69         | <b>9.9</b>   | <b>17.3</b>    | 0.07         | <b>0.06</b>  | <b>5.1</b>    | 0.7          |
| 05/24/00 | SMC   | 1.10         | <i>12.50</i> | <i>5.75</i>    | 0.08         | <i>0.55</i>  | <i>674.00</i> | <i>-0.04</i> |
| 03/16/00 | PK    | 0.62         | 0.04         | 0.10           | 0.02         | 0.06         | 1.25          | 0.82         |
| 03/28/00 | PK    | <b>168.0</b> | <b>114.0</b> | <b>1065.0</b>  | <b>366.0</b> | <b>152.0</b> | <b>1.6</b>    | <b>0.3</b>   |
| 04/25/00 | PK    | 0.01         | 0.10         | <i>39.90</i>   | 0.16         | 0.5          | <i>38.00</i>  | <i>0.58</i>  |
| 05/04/00 | PK    | <i>6.88</i>  | <b>2.6</b>   | <b>4.22</b>    | <i>0.03</i>  | <b>745.0</b> | <b>27.4</b>   | <b>0.2</b>   |

and 94% of measurement variance (Table 6) for episodes unaffected by rip currents.

As was the case for the 1D model, large values of  $D_x$  and  $D_y$  ( $\gg 1 \text{ m}^2 \text{ s}^{-1}$ ) likely compensate for loss of dye from within the surf zone by rip currents, violating the model assumption of no-flux boundaries. Accordingly, these values are excluded from analysis. Concentration magnitude and variation through time are reasonably predicted ( $R^2 > 0.6$ ) for 64% of shoreline sample stations using fitted diffusion coefficients (for example, Figure 9a - c). Note that, for 73% of sample stations  $D_y > D_x$  which is inconsistent with the earlier expectation that cross-shore mixing by wave bores exceeds alongshore mixing.

The 2D model reasonably predicts the dye patch peak concentration and in some cases the peak duration and peak asymmetry. However, neither the 1D nor 2D advection-diffusion models reproduce the concave low-concentration tail at the shoreline, suggesting that key processes responsible for this characteristic are neglected in this simple approach to dispersion modeling and estimation of dispersion coefficients in the surf zone.

Assumptions for the 2D model include no-flux of tracer at the shoreline and breaker line, no cross-shore mean velocity and no alongshore current shear ( $v \neq f(x)$ ). Field observations from this and other

studies suggest that in the absence of rip currents dye diffusion and transport is largely confined shoreward of the region of wave breaking (Harris *et al.* 1963, Inman *et al.* 1971). Furthermore, observations that dye is well mixed across the surf zone width in relatively short time may explain why alongshore spreading of dye patches has received more attention than cross-shore spreading. The apparent dominance of fitted  $D_y$  over  $D_x$  in the 2D model might at first appear consistent with assumptions for no-flux boundaries and a well mixed surf zone. However, predicted concentration time series at the shoreline lack the distinct slow decay of tracer found in measurements. Moreover, predicted concentration field in the outer surf zone is characterized by strong cross-shore concentration gradients at alongshore distances  $> 300$  m from dye release owing to estimated  $D_x \ll 1 \text{ m}^2 \text{ s}^{-1}$  but the two experiments with offshore measurements record no such gradients after  $\sim 50 - 100$  m. In the 2D model, accurately modeled peak concentration and peak width are the two most significant factors in fitting  $D_x$  and  $D_y$ . Modeled peak concentration is a function of both  $D_x$  and  $D_y$ , however, peak width is a function of  $D_y$  only. Consequently, the fit is biased toward higher  $D_y$  to approximate the peak width and  $D_x$  modifies the peak height. The alongshore persistence of tracer at the shoreline is replicated in the model by large values of  $D_y$ . The corresponding val-

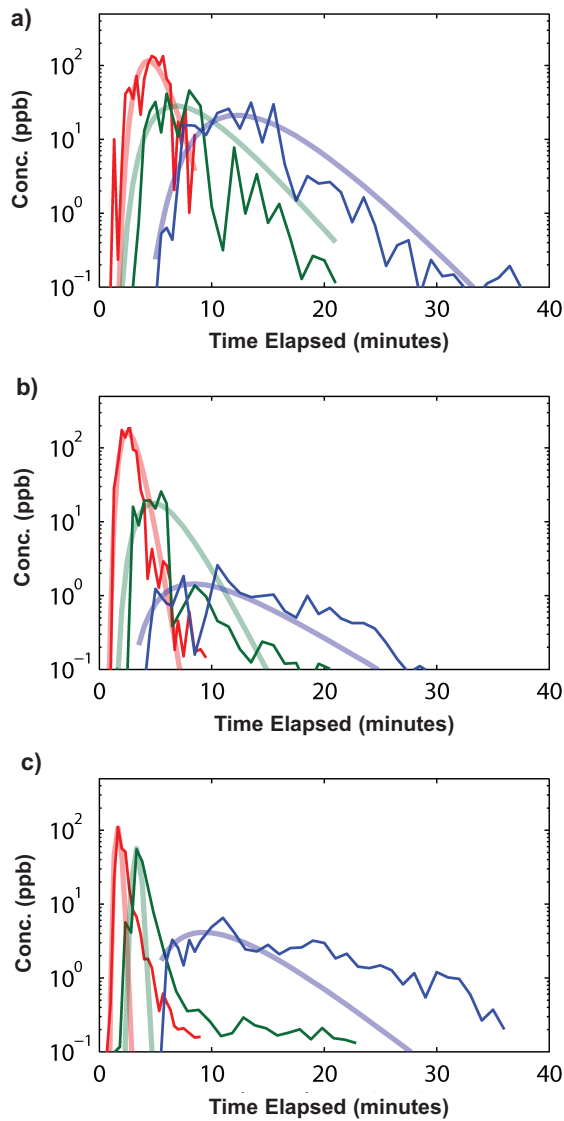


**Figure 9. Shoreline concentration time series from 2D advection-diffusion model compared to measurements at: Malibu Creek 05/24/00 (a); Pico Kenter drain 04/25/00 (b); and Santa Monica Canyon 05/04/00 (c). Measured concentration (Conc.) at 25 m (red), 50 m (green), and 100 m (blue); modeled concentration at 25 m (thick red), 50 m (thick green), and 100 m (thick blue).**

ues of  $D_x$  are an order of magnitude less than  $D_y$ , but given the expected anisotropy of mixing, enhanced in the cross-shore direction owing to turbulent passage of bores toward shore, it is difficult to justify  $D_y \gg D_x$ .

#### *Numerical solution to 2D advection-diffusion equation with alongshore current shear*

As water is transported within circulation cells, and exchanged between cells and offshore water mass, effluent introduced into the surf zone at the shoreline is diluted with ocean water through mixing

by turbulence from breaking waves and shared flow. In the context of sheared flow, the effects of molecular diffusion and turbulent mixing have been shown to increase apparent diffusion; an effect parameterized by the dispersion coefficient (Taylor 1953, 1954; Fischer 1978). Within the surf zone, the dispersion of momentum is dominated by sheared flow arising from divergent alongshore and cross-shore currents rather than by turbulent mixing (Svendsen and Putrevu 1994) and a similar effect might be expected for dispersion of land-based runoff.

Tracer dispersion is enhanced in sheared flows because small differences between tracer particle trajectories in the direction of velocity gradient result in increasing separation of those particles (Taylor 1953, 1954; Fischer 1978). In the surf zone alongshore currents may be driven by obliquely incident waves, alongshore variation in wave height or bathymetry and are frequently characterized by cross-shore variation in flow speed, the profile of which is a complex function of wave field, bathymetry and bottom roughness. On a planar beach, measurements and theory confirm a mid-surf zone maximum in wave-driven alongshore velocity decreasing rapidly to zero near the shoreline and gradually decaying to zero over a distance 0.5 - 2 times the surf zone width beyond the region of wave breaking (Longuet-Higgins 1970, Thornton and Guza 1986). The presence of sand bars or irregular bathymetry may introduce several velocity maxima in the vicinity of sand bar crests, velocity minima in troughs and a significant non-zero flow close to the shoreline (Ruessink *et al.* 2001). Given this complexity and the absence of relevant physical measurements in this field study, no attempt is made to estimate alongshore current profiles across the surf zone. Instead, the role of alongshore current shear and its effect on shoreline dye concentration at a simple hypothetical beach is investigated by numerical solution (finite difference) of the 2D advection-diffusion equation with a prescribed alongshore current velocity profile,  $v(x)$  having maximum velocity  $v_{max}$ .

Dye concentration in the surf zone,  $C(x,y,t)$ , is computed by solving the 2D advection-diffusion equation using an explicit finite difference method (first upwind difference). Alongshore velocity,  $v$ , is a smooth function of cross-shore distance,  $x$ , assuming planar bathymetry (from Thornton and Guza 1986; Figure 10).  $v_{max}$  is constant and chosen to best align simulated and measured patch front arrival times at 25, 50, and 100 m. Surf zone width ( $W$ ; Table 2) is

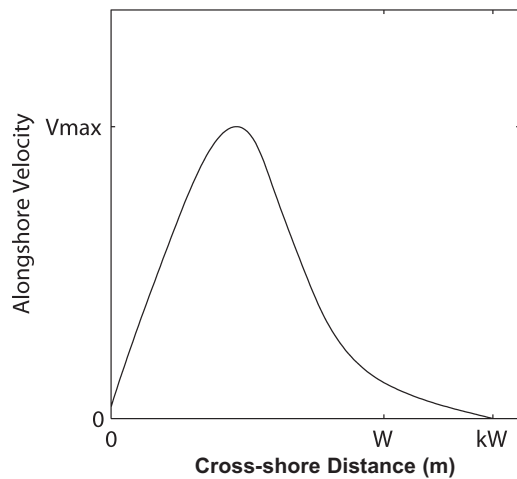


**Figure 10. Theoretical cross-shore variation in alongshore current speed for a planar beach (Thornton and Guza 1986).**

assumed to be constant alongshore as is mean surf zone depth. Dye tracer is introduced as a point source at the shoreline and there is a no-flux condition at the shoreline and breaker line.

Without measurements of alongshore current shear, numerical model results and measurements can only be compared qualitatively. Consequently, the model was run with various values of  $D_y$ ,  $D_x$ , and  $W$  to examine their effect on shoreline concentration.

Numerical model runs (including alongshore current shear) using  $D_x$  and  $D_y$  values estimated with the 2D analytical model (Table 6) resulted in only a moderate increase in peak duration. Shear-enhanced dispersion requires mixing across the region of shear but with  $D_x$  generally  $\ll 1 \text{ m}^2 \text{ s}^{-1}$  and  $D_y \gg D_x$ , the effect of alongshore current shear was only apparent at the shoreline for large elapsed times and distances alongshore (e.g.,  $W^2/4D_x \approx 90$  minutes for  $W = 25 \text{ m}$  and  $D_x = 0.03 \text{ m}^2 \text{ s}^{-1}$ ). For comparison, persistent low concentrations characterized measured shoreline concentration time series at most sites at alongshore distances as short as 25 m only 3 - 5 minutes after dye release, suggesting that for  $W = 25 \text{ m}$ ,  $D_x \approx 0.5 - 0.8 \text{ m}^2 \text{ s}^{-1}$ .

In contrast to the 2D analytical model with no alongshore current shear, the numerical model with shear more accurately reproduces the concave characteristic of shoreline concentration time series when  $D_x \gg D_y$  (Figure 11). This switch in dominance between  $D_x$  and  $D_y$  from the no-shear case illustrates the importance of alongshore current shear in surf zone dispersion and illustrates the combined effect of cross-shore mixing and alongshore current shear on

shoreline concentration measurements that cannot be duplicated in these models by simply increasing  $D_y$ .

Cross-shore mixing by waves across a region of alongshore current shear results in alongshore extension of the dye patch independent of the magnitude of  $D_y$ . The effective alongshore diffusion owing to this process increases through time and with increasing alongshore distance from the dye release point. In the 1D and 2D analytical models there is no alongshore current shear and since alongshore extension of the dye patch is controlled in those models solely by  $D_y$ , the magnitude of  $D_y$  might be expected to increase with increasing distance from dye release point to account for shear enhanced dispersion. For cases where rip currents were not observed, all but one show an increase in estimated  $D_y$  with increasing  $y$ . This trend is absent in estimated  $D_x$ .

Trying several variants of alongshore current profile in the model showed that persistent, low-concentration at the shoreline was influenced mostly by the presence of a zone of fluid with  $v \ll v_{max}$  shoreward of the breakerline which detained a fraction of the tracer while the remaining fraction was advected alongshore. Subsequent to alongshore advection of the patch peak by  $v_{max}$ , tracer detained near the breaker line gradually diffused toward the shoreline.

Alongshore current shear provides a reasonable

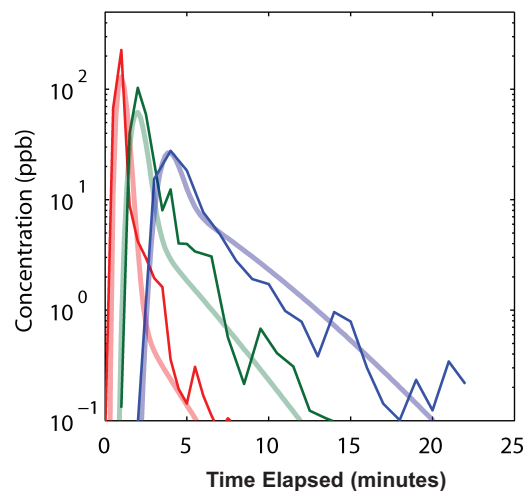


**Figure 11. Shoreline concentration time series from 2D advection-diffusion model compared to measurements at Santa Monica Canyon 03/16/00. Measured concentration at 25 m (red), 50 m (green), and 100 m (blue); modeled concentration at 25 m (thick red), 50 m (thick green), and 100 m (thick blue). Model parameters:  $D_x = 0.4 \text{ m}^2 \text{ s}^{-1}$ ,  $D_y = 0.03 \text{ m}^2 \text{ s}^{-1}$ , maximum alongshore current velocity ( $v_{max}$ ) =  $0.6 \text{ m s}^{-1}$ ,  $W = 22 \text{ m}$ .**

explanation of the concave trailing profile in time series of shoreline dye concentration for 7 out of 14 episodes. Of the remaining seven episodes, five differ in that between 25 and 50 m, or between 50 and 100 m a rip current was observed at the site and the concentration peak at the downstream sample station is up to an order of magnitude lower than at the same time and position at sites where rips were not observed. Furthermore, measured concentration time series show that following interaction between the dye patch and rip current the shoreline concentration is remarkably constant for periods up to 30 minutes with concentrations up to an order of magnitude larger than at the same time and position at sites where rips were not observed.

The observed persistence of low concentrations at the shoreline associated with rip currents is plausibly explained by offshore transport of a dye plug by rip currents, detention near the surf zone outer boundary and subsequent gradual release back into the surf zone and mixing toward the shoreline (Grant *et al.* 2005). Other possible mechanisms include retention of the dye patch by almost zero velocity alongshore current or presence of an approximately stationary eddy within the surf zone throughout which the dye is well mixed. Estimates of alongshore current velocity from dye patch advection speeds and the arrival at each sample station of generally steep patch fronts suggest that alongshore current velocity are unlikely to be zero over intervals of 10 - 30 minutes. The occurrence of slow-moving or stationary eddies have been documented in the inner surf zone (Schmidt 2003), some associated with rip currents (MacMahan *et al.* 2004). There were insufficient measurements or observations from our beach sites to comment on the role of eddies in affecting shoreline dye concentration. Instead, we use an alternative modeling approach to investigate the possible effects on shoreline concentration of dye transport offshore by rip currents and subsequent release back into the surf zone. A particle tracking model traced the trajectories of discrete fluid/tracer parcels through a prescribed surf zone flow field in which an alongshore current is interrupted by a rip current directed offshore.

#### *Particle tracking model with alongshore current shear and rip current*

A large number ( $1 \times 10^4 - 1 \times 10^5$ ) of discrete particles each representing a mass of tracer were released at the shoreline of a model domain in which

a mass conserving flow field was prescribed on a grid with spacing 2 m in  $x$  and 4 m in  $y$ . The flow field represents an idealized alongshore current transected by a rip current extending from the shoreline to beyond the outer surf zone boundary. The along shore velocity component is described by the cross-shore profile,  $v(x)$  (Figure 10). A rip current is introduced at  $y = y_{rip}$  with width,  $\Delta y_d$ . In the region  $y_{rip} \leq y \leq y_{rip} + \Delta y_d$ ,  $v(x)$  smoothly decelerates to  $fv(x)$ , where  $f < 1$ . Immediately downdrift from the rip current,  $v(x)$  smoothly accelerates over a distance  $\Delta y_a$ , ( $\Delta y_a \gg \Delta y_d$ ), after which  $v(x)$  has maximum  $v_{max}$ . Once  $v$  is defined on the grid, cross-shore velocity,  $u(x,y)$  is computed as:

$$u(x, y) = -\frac{1}{d(x)} \int_{x_0}^x \frac{\partial vd}{\partial y} dx \quad (7)$$

where  $d(x)$  is the water depth assumed to increase monotonically offshore to a distance  $kW$  beyond which the offshore directed rip velocity is rapidly slowed by artificially increasing the depth exponentially. The resulting flow field exhibits a narrow offshore directed jet dissipating offshore and a gradually accelerating alongshore current downdrift of the rip being fed by low velocity onshore flow (see Figure 13a for an example flow field). The flow field is not intended to represent any particular site but rather to explore the primary effect of rip current flow on shoreline dye concentration. Particle position was updated every time-step,  $\Delta t = 1$  sec, as the sum of advective ( $\bar{U}(x,y)\Delta t$ ) and diffusive ( $L_x, L_y$ ) displacements.

$$\Delta x = U_x \Delta t + L_x, L_x = [r]_{-1}^1 \sqrt{6D_x \Delta t} \quad (8)$$

$$\Delta y = U_y \Delta t + L_y, L_y = [r]_{-1}^1 \sqrt{6D_y \Delta t} \quad (9)$$

where  $U_x$  and  $U_y$  are the cross-shore and alongshore advection velocities bilinearly interpolated at particle positions in the flow field and  $[r]$  is a random number in the interval  $[-1,1]$  (Sanchez Arcilla *et al.* 1998). Shoreline concentration time series,  $C(x = 0, y, t)$ , were predicted with the model with particle density related to concentration (ppb) according to:

$$C(x = 0, y, t) = \frac{pM}{d_x d_y P} \times 10^6, \quad (10)$$

where  $p$  is number of particles in sample area  $d_x \times d_y$ ,  $M$  is dye mass (kg) and  $P$  is the total number of particles released.

Without a rip current the flow field is defined by three parameters,  $W$ ,  $k$  and  $v_{max}$ .  $W$  is not a free parameter but fixed as the lower estimated surf zone width from Table 2 for each day. The value of  $v_{max}$  is a constant constrained by the alignment of simulated and measured patch front arrival times at 25, 50, and 100 m. The model was tuned using three free parameters ( $k$ ,  $D_x$  and  $D_y$ ) with the aim of reproducing characteristics of measured concentration time series. The position of a rip current is fixed as the observed alongshore distance from the dye release point. The strength and offshore extent of a rip current is defined by four parameters,  $k$ ,  $f$ ,  $\Delta y_d$  and  $\Delta y_a$ . Deceleration of the alongshore current determines the rip strength and is the primary factor governing the removal of particles from the surf zone and the maximum concentration downstream of the rip. Although the rate of particle entrainment back into the surf zone depends on the offshore extent of the rip, the acceleration distance of  $v$  and offshore diffusion coefficients (fixed for all runs as  $D_x = D_y = 0.03 \text{ m}^2 \text{ s}^{-1}$ ; Wood *et al.* 1993), these parameters affect the concentration magnitude but not the general characteristic of persistent low concentrations at the shoreline downdrift from the rip current.

The model simulated shoreline concentration time series comparable with measurements at several of the sites without rip currents (e.g., Figure 12a - c) and with rip currents (e.g., Figure 12d).

At Malibu Creek (03/28/00 and 05/24/00; Figure 12a and b)  $D_x \approx D_y$  yielded the best model fit consistent with the generally high angle of wave incidence at that site causing waves to break from west to east so that mixing associated with wave breaking is likely to have a significant alongshore component. In addition, best agreement between model and measurements was obtained for  $v(1.4W) = 0$  at Malibu Creek, whereas  $v(1W) = 0$  at Santa Monica Canyon and Pico Kenter drain.

In contrast to Malibu Creek the model approximated shoreline concentration time series at Santa Monica Canyon (03/16/00, no observed rip current) with  $D_x = 1.5 \text{ m}^2 \text{ s}^{-1}$ ,  $D_y = 0.08 \text{ m}^2 \text{ s}^{-1}$ ,  $k = 0.85$  and  $v_{max} = 0.7 \text{ m s}^{-1}$  (Figure 12c). At Santa Monica Canyon on 05/04/00 a rip current was observed 70 m alongshore from the dye release point. Modeled shoreline concentration time series reflect both magnitude

and shape of measured shoreline time series (Figure 12d) with  $D_x = 0.25 \text{ m}^2 \text{ s}^{-1}$  and  $D_y = 0.025 \text{ m}^2 \text{ s}^{-1}$ . In the model, emerging from the rip current prior to leaving the surf zone (Figure 13a). In the region offshore from the breaker line particles dispersed isotropically, some of which re-entered the surf zone. After 40 minutes, about half the particles remained in a mass outside the breaker line (Figure 13b); consistent with estimates by Inman *et al.* (1971).

The magnitude of  $D_x = 1.5 \text{ m}^2 \text{ s}^{-1}$  at Santa Monica Canyon on 03/16/00 is relatively large and tracer concentration at the breaker line reaches levels equal to shoreline concentration very rapidly ( $y < 30 \text{ m}$ ). Episodes where samples were collected at the breaker line (Malibu Creek 06/07/00 and Pico Kenter drain 06/07/00) showed the ratio between shoreline and breaker line concentration to be about 100:1 at 25 m, and 10:1 or less at 50 m. Cross-shore variations in velocity and dispersion coefficient more complex than applied here are likely to result from pronounced sand bar and trough bathymetry along with associated wave breaking and wave reforming.

## RESULTS

### Implications for Continuous Injection Events

Although many details of the physical environment are unknown, reasonable parameter values in the particle tracking model results in predictions of shoreline dye concentration both qualitatively and quantitatively similar to measurements. Ideally, additional measurements of offshore concentration and flow characteristics would allow model verification. However, in the light of the apparent agreement between the model and measurements, the model was extended to investigate the potential effects on shoreline concentration of continuous effluent release into the surf zone.

The model was run for two flow scenarios; first without a rip current; second, a rip current located 70 m from the particle release point. In both cases 25 particles were released per time step (1 second) for a duration of 0.5 hours (simulating a contaminant release rate of  $0.025 \text{ kg hr}^{-1}$ ). The model was run for two hours.

In both cases, within 5 min shoreline concentration at 25 and 50 m had increased 40 – 50 ppb which remained constant until the last particles released at the source reached the sample stations ( $t \approx 30 \text{ minutes}$ ). For the case with no rip current, shoreline concentration reached a maximum of 40 ppb within 15 m. Shortly after particle release ceased, the concentration decreased rapidly to  $< 0.1 \text{ ppb}$  within 5 minutes at 25 m,

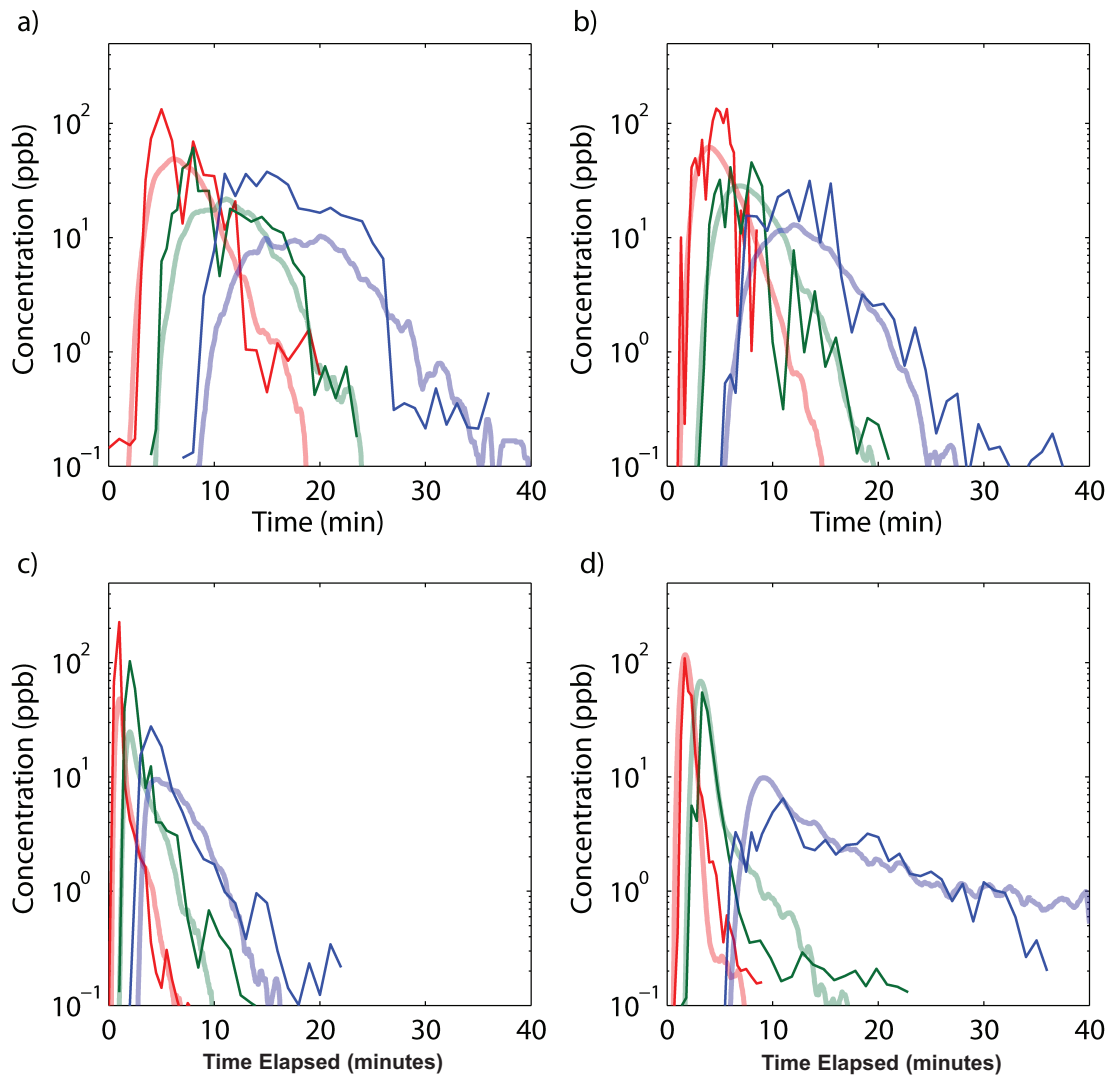


**Figure 12.** Shoreline concentration time series from particle tracking model (thick lines) compared to measurements (thin lines) at 25 m (red), 50 m (green), and 100 m (blue). Malibu Creek 03/28/00 - Model parameters:  $D_x = 0.08 \text{ m}^2 \text{ s}^{-1}$ ,  $D_y = 0.04 \text{ m}^2 \text{ s}^{-1}$ ,  $W = 25 \text{ m}$ ,  $k = 1.4$ ,  $v_{max} = 0.22 \text{ m s}^{-1}$ , 20,000 particles,  $M = 0.75E - 2 \text{ kg dye}$  (a); Malibu Creek 05/24/00 - Model parameters:  $D_x = 0.11 \text{ m}^2 \text{ s}^{-1}$ ,  $D_y = 0.11 \text{ m}^2 \text{ s}^{-1}$ ,  $W = 25 \text{ m}$ ,  $k = 1.45$ ,  $v_{max} = 0.33 \text{ m s}^{-1}$ , 20,000 particles,  $M = 1.05E - 2 \text{ kg dye}$  (b); Santa Monica Canyon 03/16/00 - Model parameters:  $D_x = 1.5 \text{ m}^2 \text{ s}^{-1}$ ,  $D_y = 0.08 \text{ m}^2 \text{ s}^{-1}$ ,  $W = 24 \text{ m}$ ,  $k = 0.85$ ,  $v_{max} = 0.7 \text{ m s}^{-1}$ , 20,000 particles,  $M = 1.05E - 2 \text{ kg dye}$  (c); and Santa Monica Canyon 05/04/00 for a rip current located 70 m from dye release point - Model parameters:  $D_x = 0.25 \text{ m}^2 \text{ s}^{-1}$ ,  $D_y = 0.03 \text{ m}^2 \text{ s}^{-1}$ ,  $W = 19 \text{ m}$ ,  $k = 0.9$ ,  $v_{max} = 0.45 \text{ m s}^{-1}$ , 60,000 particles,  $M = 1.2E - 2 \text{ kg dye}$  (d). Rip current parameters:  $k = 1.1$ ,  $f = 0.3$ ,  $\Delta y_d = 8 \text{ m}$  and  $\Delta y_a = 75 \text{ m}$ . Outside the surf zone  $D_x = D_y = 0.03 \text{ m}^2 \text{ s}^{-1}$ .

12 minutes at 50 m, and 22 minutes at 100 m. For the rip current case, starting at  $t \approx 9$  minutes, shoreline concentration at 100 m increased gradually to a maximum of 20 ppb at  $t = 37$  minutes then decayed approximately exponentially to  $\approx 1$  ppb over two hours (Figure 14 a).

Without a rip current the predicted shoreline concentration at  $t = 120$  minutes exceeds 0.1 ppb over 1150 m of shoreline with a maximum concentration of 13 ppb with the tracer patch being approximately symmetrical alongshore. In contrast, when

the rip current is present the predicted shoreline concentration at  $t = 120$  minutes exceeds 0.1 ppb over 1450 m of shoreline with a maximum concentration of 3 ppb (Figure 14 b). In the model, the presence of a rip current reduced the maximum shoreline tracer concentration by an order of magnitude for a discrete particle release, but only by a factor of  $\sim 2$  for a continuous release. In both cases the rip current at least doubled the duration and alongshore extent for shoreline contamination.

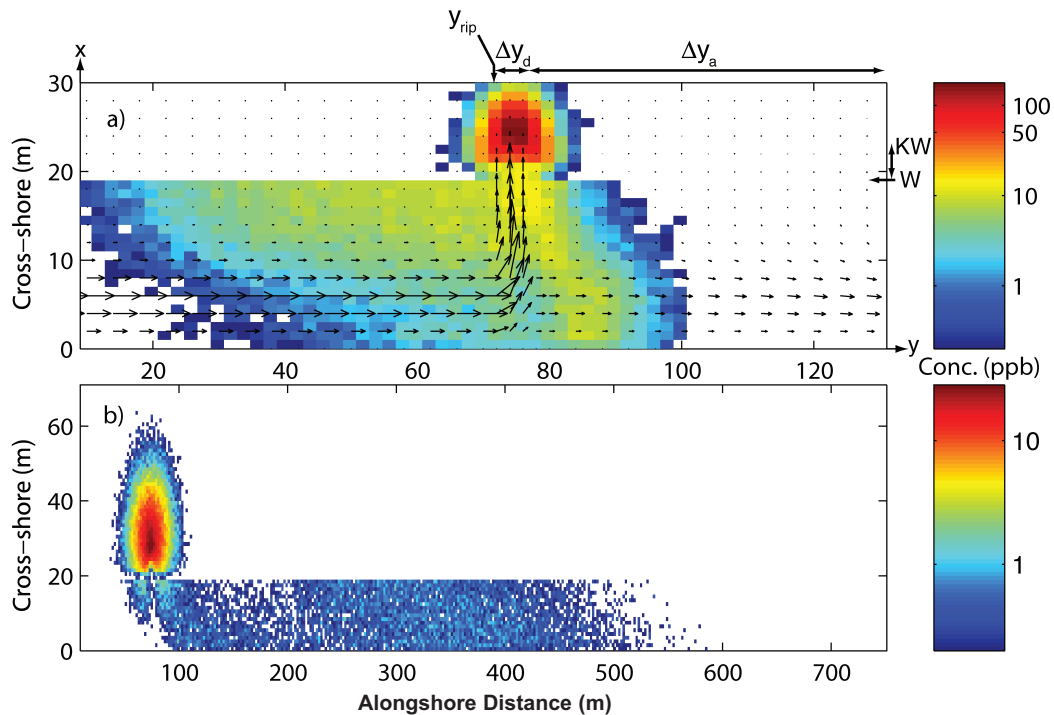


**Figure 13. Simulated concentration field from particle tracking model for Santa Monica Canyon on 04/05/00: 7 minutes (a) and 40 minutes (b) after particle release. Vectors show alongshore current shear ( $v_{max} = 0.45 \text{ m s}^{-1}$ ) and rip current located at 70 m alongshore. Surf zone width = 19 m.**

## DISCUSSION

Although these measurements of dye patch dispersion in the surf zone are limited to the shoreline they reveal the effects of various surf zone flow conditions on the extent and duration of beach contamination. Despite inadequate physical measurements quantifying flow conditions the simple models presented in this paper demonstrate plausible relationships between distinct characteristics of the shoreline dye concentration time series and flow properties of alongshore current shear and rip currents.

Alongshore spreading of dye is enhanced by alongshore current shear in conjunction with cross-shore wave-driven mixing, and regions of slower-moving flow result in retention of traces of dye at the shoreline long after the main dye patch has advected past. Dye entrained in offshore-directed rip currents is advected into waters beyond the region of wave breaking after which it maybe gradually reintroduced into the surf zone causing persistent low concentration at the shoreline. Both of these flow properties are just two of many possible mechanisms resulting in retention of dye in regions of low velocity flow or reduced mixing. For example, dye retention was observed in slow-moving shallow water amongst rocks at Malibu Creek (05/24/00) which was gradu-

ally mixed and entrained into alongshore flow resulting in the persistence of dye at 50 and 100 m up to 20 - 35 minutes after release. At Santa Monica Canyon (3/28/00), the dye patch was observed being transported offshore beyond the breakers in a rip current at  $y \approx 0 \text{ m}$ , gradually feeding back into the surf zone while advecting slowly alongshore. At Santa Monica Canyon (05/24/00), a sand bar was observed  $\approx 20 \text{ m}$  offshore in water depth  $\approx 0.3 \text{ m}$  separated from the shoreline by a 1.5 m deep trough. All dye appeared to remain shoreward of the sand bar, but shoreline concentration time series at 25, 50, and 100 m all show broad dye patches with low peak concentration despite the largest dose of dye used in all batch release episodes (50 ml fluorescein). Wave breaking over the sand bar and wave-reformation in the trough would likely result in cross-shore gradients in wave-driven mixing ( $D_x$ ) and alongshore current velocity with a minimum within the trough (Ruessink *et al.* 2001) where dye might be retained.

In addition to alongshore current shear and rip currents, near-bed, offshore flow (undertow) may give rise to significant flow shear in the vertical direction, which, combined with vertical turbulence, is likely to enhance cross-shore mixing. Strong concentration gradients just offshore of the region of

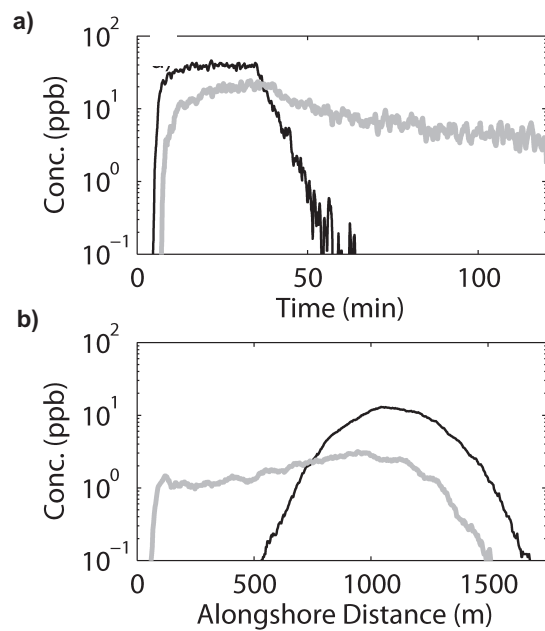


**Figure 14. Rip current effects on shoreline concentration predicted when particles are released continuously for the first 30 minutes of a 120-minute model run: concentration at 100 m alongshore from release point – without rip current, indicated by the black line, and with a rip current at 70 m, indicated by the gray line (a); alongshore concentration at the shoreline at  $t = 120$  minutes – without rip current is indicated by the black line and with a rip current at 70 m indicated by the gray line (b). Flow field and model parameters identical to those in Figure 12d.**

wave breaking observed in this and other studies (Harris *et al.* 1963, Inman *et al.* 1971, Bowen and Inman 1974) suggest tracer flux out of the surf zone is much less than cross-shore flux inside the surf zone. In this work a no-flux condition at the surf zone offshore boundary was assumed except near rip currents, however, undertow extending some distance beyond the breaker line (Putrevu and Svendsen 1993, Garcez Faria *et al.* 2000) may result in a significant dye flux at the edge of the surf zone.

Mixing of dye from the region of relatively slow alongshore current near the surf zone boundary into deeper water beyond the surf zone and the mixing of dye ejected from the surf zone by rip currents back into the surf zone are of primary importance for transport and fate of surf zone contaminants and the extent in time and space of their impact at the shoreline, but the processes affecting mass exchange between the surf zone and ambient coastal waters are not well understood. Furthermore, because shore-parallel currents are typically wave-driven within the surf zone and wind and tidally driven offshore, dye

advected beyond the breaker line may be transported in the opposite direction to flow within the surf zone with the potential to contaminate shoreline upstream from the original contaminant source.

Tidally modulated translation of the surf zone in the cross-shore direction may cause contaminants mixed to the offshore extent of the surf zone during low tide to disperse relatively slowly during high tide. On a subsequent low tide this stranded contaminant might be reintroduced to the surf zone and act as a source of shoreline contamination in addition to land-based sources.

The offshore plume resulting from a single rip current may act as slow release contaminant source at the offshore surf zone boundary. Each successive rip current acts to create similar, but progressively lower concentration sources resulting in a significantly longer contaminant residence time near the shoreline.

Estimates of  $D_y$  from the 1D advection-diffusion model ranged 0.003 - 0.5 m<sup>2</sup> s<sup>-1</sup>, consistent with values from literature. However, for instances unaffected by rip currents and potential dye loss from the surf zone, shoreline concentration time series simulated using estimated  $D_y$  showed concentration peaks much shorter than measurements. For instances where rips were observed, the decrease in concentration due to the dye loss from the surf zone was reproduced in the models by increasing alongshore mixing. This resulted in exaggerated estimates of  $D_y$  and unrealistic alongshore stretching of the dye patches.

Estimates of diffusion coefficients from the 2D advection-diffusion model without alongshore current shear for instances unaffected by rip currents ranged 0.003 - 0.9 m<sup>2</sup> s<sup>-1</sup> for  $D_x$  and 0.004 - 1.35 m<sup>2</sup> s<sup>-1</sup> for  $D_y$ . Simulated shoreline dye concentration time series explained between 66 - 94% of variance in measurements but failed to reproduce the characteristic concave profile following the peak in concentration time series. Iterative runs of a numerical 2D advection diffusion model incorporating alongshore current shear consistently estimated  $D_x \gg D_y$ , illustrating the combined importance of cross-shore mixing and alongshore shear in alongshore spreading of the dye patch. Furthermore, inclusion of alongshore current shear resulted in simulated shoreline concentration time series with concave profile similar to measurements. In the model, the concave profile resulted from cross-shore mixing of dye into regions of slower moving flow followed by remixing of dye back toward the shoreline after the main patch had been advected alongshore.

Shoreline concentration time series for 7 of 14 dye release episodes were characterized by low dye concentrations persistent over 20 - 30 minutes despite non-zero alongshore current velocities. Although a variety of surf zone flow patterns might lead to dye retention or recirculation, visual observations of rip currents were associated with five of the episodes. A particle tracking model for 2D advection-diffusion was used to simulate shoreline dye concentration time series for an idealized surf zone flow field with alongshore current transected by a rip current. Simulated shoreline dye concentration time series for actual dye doses and observed rip current positions compare favorably with measured peak duration, dilution and concentration profile. Measurements and model results suggest that the presence of a rip current may reduce the maximum shoreline concentration by a factor of 10 for a discrete dye release, but only by a factor 2 - 3 for continuous dye release. In both cases, the presence of a rip current may increase the duration and alongshore extent for shoreline contamination by a factor of two or more.

## LITERATURE CITED

- Allen, J.S., P.A. Newberger and R.A. Holman. 1996. Nonlinear shear instabilities of alongshore currents on plane beaches. *Journal of Fluid Mechanics* 310:181-213.
- Boehm, A.B. 2003. Model of microbial transport and inactivation in the surf zone and application to field measurements of total coliform in northern Orange County, California. *Environmental Science and Technology* 37:5511-5517.
- Boehm, A.B., D.P. Keymer and G.G. Shellenbarger. 2005. An analytical model of enterococci inactivation, grazing, and transport in the surf zone of a marine beach. *Water Research* 39:3565-3578.
- Boehm, A.B., G.G. Shellenbarger and A. Paytan. 2004. Groundwater discharge: Potential association with fecal indicator bacteria in the surf zone. *Environmental Science and Technology* 38:3558-3566.
- Bowen, A.J. and D.L. Inman. 1974. Nearshore mixing due to waves and wave induced currents. *Rapports et process-verbaux des reunions Commission internationale pour l'exploration scientifique de la Mer Méditerranée* 167:6-12.
- Fischer, H.B. 1978. On the tensor form of the bulk dispersion coefficient in abounded skewed shear flow. *Journal of Geophysical Research* 83:2373-2375.
- Fischer, H.B., E.J. List, R.C. Y. Koh., J. Imberger and N. Brooks. 1979. Mixing in inland and coastal waters. Academic Press. New York, NY.
- Garcez Faria, A.F., E.B. Thorton, T.C. Lippmann and T.P. Stanton. 2000. Undertow over a barred beach. *Journal of Geophysical Research* 105:16999-17010.
- Grant, S.B., J.H. Kim, B.H. Jones, S.A. Jenkins, J. Wasyl and C. Cudaback. 2005. Surf zone entrainment, along-shore transport, and human health implications of pollution from tidal outlets. *Journal of Geophysical Research* 110:C10025-C10045.
- Grant, S.B., B.F. Sanders, A.B. Boehm, J.A. Redman, J.H. Kim, R.D. Mre, A.K. Chu, M. Gouldin, C.D. McGee, N.A. Gardiner, B.H. Jones, J. Svejksky, G.V. Leipzig and A. Brown. 2001. Generation of enterococci bacteria in a coastal saltwater marsh and its impact on surf zone water quality. *Environmental Science and Technology* 35:2407-2416.
- Harris, T.F. W., J.M. Jordaan, W.R. McMurray, C.J. Verwey and F.P. Anderson. 1963. Mixing in the surf zone. *International Journal of Air and Water Pollution* 7:649-667.
- Inman, D.L., F.J. Tait and C.E. Nordstrom. 1971. Mixing in the surf zone. *Journal of Geophysical Research* 76:3493-3514.
- Komar, P.D. 1998. Beach Processes and Sedimentation, 2nd Edition. Prentice-Hall International. London, UK.
- Longuet-Higgins, M.S. 1970. Longshore currents generated by obliquely incident sea waves, parts 1 and 2. *Journal of Geophysical Research* 75:6778-6780.
- MacMahan, J.H., A.J. Reniers, E.B. Thornton and T.P. Stanton. 2004. Surf zone eddies coupled with rip current morphology. *Journal of Geophysical Research* 109:C07004-C07019.
- Murray, A.B. and G. Reydellet. 2001. A rip current model based on a hypothesized wave/current interaction. *Journal of Coastal Research* 17:517-530.
- Noble, R.T., J.H. Dorsey, M.K. Leecaster, V. Orozco-Borbon, D. Reid, K.C. Schiff and S.B. Weisberg. 2000. A regional survey of the microbiological

- water quality along the shoreline of the Southern California Bight. *Environmental Monitoring and Assessment* 64:435-447.
- Ozkan-Haller, H.T. and J.T. Kirby. 1999. Nonlinear evolution of shear instabilities of the longshore current: a comparison of observations and computations. *Journal of Geophysical Research* 104:25953-25984.
- Putrevu, U. and I. A. Svendsen. 1993. Vertical structure of the undertow outside the surf zone. *Journal of Geophysical Research* 98:22707-22716.
- Ruessink, B.G., J.R. Miles, F. Feddersen, R.T. Guza and S. Elgar. 2001. Modeling the alongshore current on barred beaches. *Journal of Geophysical Research* 106:22451-22463.
- Sanchez-Arcilla, A., A. Rodriguez and M. Mestres. 1998. A three-dimensional simulation of pollutant dispersion for the near and far-field in coastal waters. *Journal of Marine and Environmental Engineering* 4:217-243.
- Schiff, K.C., J. Morton and S.B. Weisberg. 2003. Retrospective evaluation of shoreline water quality along santa monica bay beaches. *Marine Environmental Research* 56:245-254.
- Schmidt, W.E. 2003. Lagrangian Observations of Surfzone Currents. University of California, San Diego. San Diego, CA.
- Shepard, F.P. and D.L. Inman. 1951. Nearshore circulation. pp. 50-59 in: Proceedings of the First Conference on Coastal Engineering, Council on Wave Research. Berkley, CA.
- Slinn, D.N., J.S. Allen, P.A. Newberger and R.A. Holman. 1998. Nonlinear shear instabilities of alongshore currents over barred beaches. *Journal of Geophysical Research* 103:18357-18379.
- Smart, P.L. and I.M.S. Laidlaw. 1977. An evaluation of some fluorescent dyes for water tracing. *Water Resources Research* 13:15-32.
- Smith, J.A. and J.L. Largier. 1995. Observations of nearshore circulation: rip currents. *Journal of Geophysical Research* 100:10967-10975.
- Stretch, D. and D. Mardon. 2005. A simplified model of pathogenic pollution for managing beaches. *Water SA* 31:47-52.
- Svendsen, I.A. and U. Putrevu. 1994. Nearshore mixing and dispersion. *Proceedings of the Royal Society of London Series A* 445:561-576.
- Taylor, G.I. 1953. Dispersion of soluble matter in solvent flowing slowly through a tube. *Proceedings of the Royal Society of London Series A* 219:186-203.
- Taylor, G.I. 1954. The dispersion of matter in turbulent flowing through a pipe. *Proceedings of the Royal Society of London Series A* 223:446-468.
- Thornton, E.B. and R.T. Guza. 1986. Surf zone longshore currents and random waves: Field data and models. *Journal of Physical Oceanography* 16:1165-1178.
- Wood, I., R. Bell and D. Wilkinson. 1993. Ocean Disposal of Waste Water. Advanced Series on Ocean Engineering. Ithaca, NY.

## ACKNOWLEDGMENTS

The authors are grateful to Dario Diehl and Liesl Tiefenthaler (both at Southern California Coastal Water Research Project) for assistance in field sampling. This study was supported by the City of Los Angeles and Los Angeles Regional Water Quality Control Board and the Quest for Truth Foundation.